EREM 79/1
Journal of Environmental Research, Engineering and Management
Vol. 79 / No. 1 / 2023
pp. 90–109
DOI 10.5755/j01.erem.79.1.32576

Optimization Applying Response Surface Methodology in the Co-treatment of Urban and Acid Wastewater from the Quiulacocha Lagoon, Pasco (Peru)

Received 2022/10 | Accepted after revision 2023/02

https://doi.org/10.5755/j01.erem.79.1.32576

Optimization Applying Response Surface Methodology in the Co-treatment of Urban and Acid Wastewater from the Quiulacocha Lagoon, Pasco (Peru)

Carmen Barreto-Pio[1,*], Luigi Bravo-Toledo[1], Paul Virú-Vásquez[2], Ana Borda-Contreras[1], Edgar Zarate-Sarapura[3], Alex Pilco[1]

[1]Faculty of Environmental Engineering and Natural Resources, National University of Callao, Peru

[2]Environmental Research and Development Area, Environmental Sciences Strategic Research Group (ENSCIENCE), Peru

[3]Faculty of Natural and Exact Sciences, National University of Callao, Peru

***Corresponding author:** cebarretop@unac.edu.pe

The co-treatment of acidic water (AW) and urban wastewater (UWW) is a technique that allows mitigating the negative impact of AW on natural aquatic environments, which represents one of the major environmental problems globally. The aim of this research was to determine the optimal conditions through the response

surface methodology (RSM) with a central composite design (CCD) for the co-treatment of AW from the Quiulacocha lagoon in Pasco and UWW from a municipality in Lima, Peru, having as factors the molar ratio of total iron (Fe_T) and total phosphorus (P_T), time (min) and stirring speed (rpm). Data processing was performed using the Design-Expert 11 software, and analysis of variance (ANOVA) with a confidence interval of 95% ($\alpha = 0.05$) was used. The statistical models obtained showed high determination coefficients (R^2), higher than 92% for pH, conductivity and Fe_T removal. While the removal of turbidity, COD, P_T and SO_4^{-2} obtained a value of R^2>0.80, as well as evidenced compliance with the level of significance *P* value >0.05. The optimal conditions determined by the statistical model were given at a Fe_T /P_T molar ratio (33:1), a stirring time of 5 min and a speed of 255 rpm. In these conditions, the COD was reduced by 71.78%, Fe_T by 99.48%, and P_T by 84.29% with a residual concentration of 1.3 mg/L; the pH obtained a value of 5.7 and the turbidity 56 NTU. Better efficiency of the co-treatment for the reduction of pollutants in the AW of the Quiulacocha lagoon is evidenced, applying an experimental design to optimize the operating conditions, taking into account that the molar ratio is a significant factor and that optimizing it would allow the co-treatment to be replicated. Co-treatment is a sustainable and promising alternative for the treatment of AW and UWW, since it does not require the use of chemical agents to treat water. However, post-treatments would still be required to comply with certain regulations or to reuse the treated water on a larger scale.

Keywords: co-treatment experiments, experimental design, jars test, total iron, total phosphorus.

Introduction

In Peru, the acidic water (AW) generated by mining tailings brings with them high concentrations of heavy metals that modify the balance of ecosystems and generate a potential health risk for humans (Zhuang et al., 2009). In areas surrounding the Quiulacocha lagoon (Pasco-Junin-Peru), mining tailings have been deposited without any treatment, containing 50% pyrite by weight, impacting local ecosystems (Baylón Coritoma et al., 2018), as well as local populations (Astete et al., 2009). These mining tailings have an extension of 114 ha, which have infiltrated the Quiulacocha lagoon generating AW with high concentrations of Fe^{+3} y Fe^{+2} (Dold et al., 2009).

Acidic water is known by having high concentrations of dissolved metals and it is considered one of the main sources of environmental pollution for water resources (Naidu et al., 2019). Iron is one of the main pollutants in AW, known by its instability and oxidation (Schippers, 2007), with dangerous and toxicology effects on aquatic and terrestrial organisms and ecosystems (Talukdar et al., 2016). On the other hand, urban wastewater (UWW) has microbial contaminants, oxyanions and nutrients (Yang et al., 2020), of which ammonia and phosphate are the elements of main ecological concern due to their ecological impact such as eutrophication (Mavhungu et al., 2020). A limited number of researches have focused on the co-treatment of AW and UWW (Carneiro Brandão et al., 2020; Edzai et al., 2020; Silva et al., 2021).

The co-treatment implies the use of elements in AW (Fe^{+3} y Al^{+3}) and divalent chemicals (Mg^{+2}, Ca^{+2} and Mn^{+2}) that have a high affinity for the phosphorus being in the UWW, promoting precipitation (Masindi et al., 2022). However, as highlighted by Ruihua et al. (2011), water from the interaction product of AW and UWW concentrations may achieve synergistic effects.

Also, the research carried out by Masindi et al. (2022) shows that Al and Fe precipitate as (oxy)-hydroxides of iron and aluminum, while phosphates are eliminated as mineral phases of Pb, Mn, Al and Fe. The sewage sludge generated in the co-treatment was dominated by Fe and P as the main elements, confirming that the interaction of AW with UWW can lead to the removal of pollutants from both wastewater streams.

The co-treatment of AW with UWW is a promising alternative that allows two types of wastewater to be treated through a single system, avoiding the use of chemical agents for the neutralization of AW and iron removal, reflecting in a reduction of sludge, operation and maintenance costs (Johnson and Younger, 2006), as well as the reduction of the area of land required for the treatment of both types of water through separate lines; considering this alternative a type of sustainable treatment (Muga and Mihelcic, 2008). Nevertheless, Masindi et al. (2022) recommends its application as a pretreatment technique due to its feasibility of co-treating AW with UWW on an industrial scale. However, the optimization of the co-treatment of these two types of wastewater would increase the efficiency as a pretreatment (Masindi et al., 2022), being necessary to improve the operating conditions of the different parameters that have a significant effect on the co-treatment (Ruihua et al., 2011), such as the initial concentrations of iron and phosphorus present in the wastewater, volume ratios, contact time, stirring speed, sedimentation and pH (Masindi et al., 2022). Researchers have reported that optimization models have experimental advantages to improve operating conditions and the analysis of different processes. (Calabi-Floody et al., 2019; Huzir et al., 2019).

Response surface methodology (RSM) is used for cross-factor interaction analysis to achieve optimal responses using the minimum number of experiments (Montgomery, 2017; Panić et al., 2015). One of the widely applied response surface methods is the composite central design (CCD). In this context, this research applied CCD to model the relationship between three independent study variables (Fe/P molar ratio, stirring time, stirring speed) and dependent or response variables (pH, conductivity, turbidity, removal of chemical oxygen demand (COD), Fe_T, P_T y SO_4^{-2}. In this sense, the objective of this study was to optimize the co-treatment of UWW and AW from the Quiulacocha lagoon through the CCD methodology.

Methods

Research area

The research area corresponds to the AW coming from the Quiulacocha lagoon (Pasco-Junin-Peru), the place where mining tailings have been deposited without any treatment, with a high content of pyrite, that infiltrates the Quiulacocha lagoon generating AW with a high concentration of Fe^{+3} y Fe^{+2} (Dold et al., 2009). In *Fig. 1*, the Quiulacocha lagoon location (359778.00 E; 8816825.00 S) and the UWW treatment plant (277345.05 E, 8675960.0 S) are shown.

Sample collection

The AW samples were collected from the Quiulacocha lagoon, located in the Simón Bolivar district, Pasco province, Pasco district as shown in *Fig. 1* at a depth of 30 cm, according to the National Protocol for Monitoring the Quality of Surface Water Resources in Peru (ANA, 2016). The samples collected from the AW were composite samples. UWW samples were collected from the equalizer tank of the wastewater treatment plant of the municipality of Independencia in Lima, Peru. The samples were collected twice a day to have a greater representativeness.

The UWW and AW samples were stored in 60 L high-density polyethylene containers at 4 °C and transferred to the laboratory of the Faculty of Environmental Engineering and Natural Resources at the National University of Callao for co-treatment tests and analysis. All the analysis were done by triplicate (n = 3).

Selection of variables

Three parameters were conditioned as variables: the molar ratio (Fe_T:$P_{T)}$ (effect of the molar ratio), the stirring time (effect of the contact time) and the stirring speed (effect of rapid mixing). The quality parameters of the water treated were pH, turbidity, chemical oxygen demand (COD), sulfates (SO_4^{-2}), total iron (Fe_T) and total phosphorus (P_T). The Fe/P molar ratio was calculated based on the following Equation (1):

$$MR = \frac{1}{V} x \frac{\frac{[Fe_T]}{W_{Fe}}}{\frac{[P_T]}{W_P}} \quad (1)$$

Where: MR – Molar ratio (L); [ ] – concentration; V – volume of the solution (L).

Fig. 1. *Location of the sampling sites of the AW and UWW*

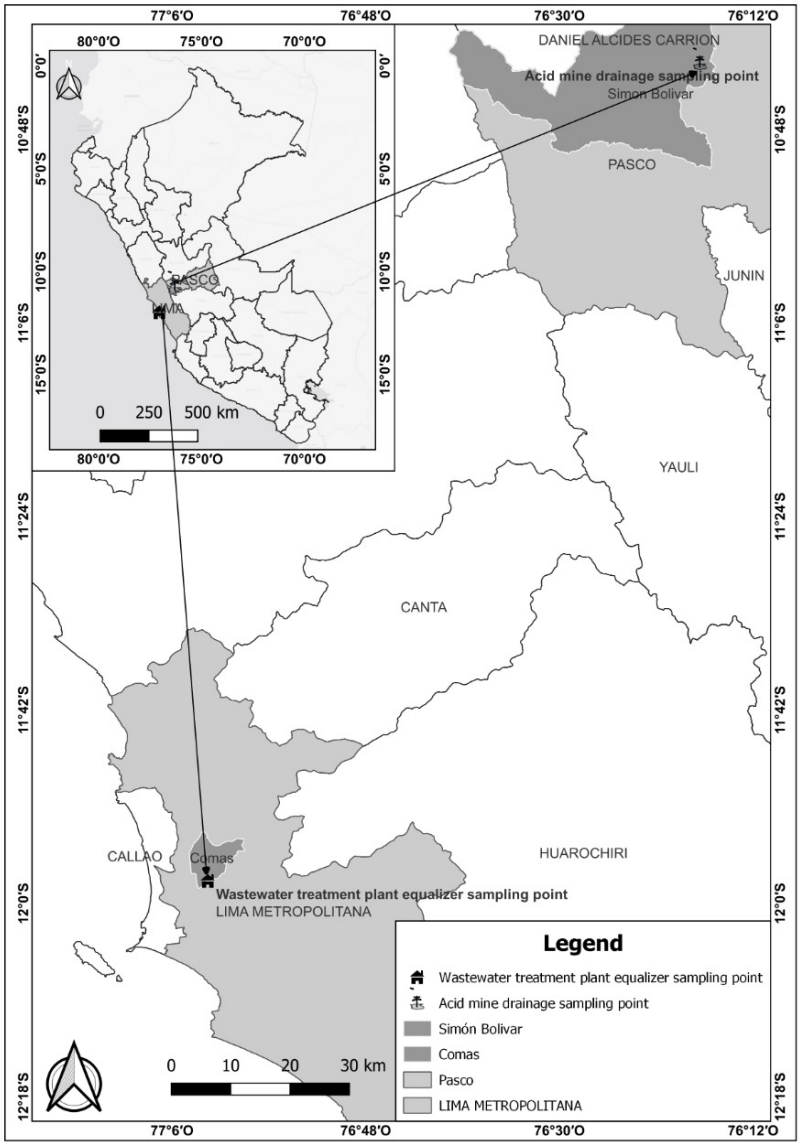

Jar test

The co-treatment tests were carried out mixing the AW with the UWW at different dosages of Fe_T/P_T molar ratios in a one-liter beaker, varying the mixing times and the stirring speed. After the mixing process, the samples were allowed to settle, taking the clarified part for the determination of the corresponding parameters. The equipment used for the experimental development was a jar tester (WiseStir Jar Tester Wisd model) equipped with six variable speed stirrers with an illuminator, as shown in *Fig. 2*. Each beaker was filled with 1 L according to the different dosages between AW and UWW.

Dosages were added according to the molar ratio (mmol Fe_T/mmol P_T) in a range from 25 to 40, to each 1 L beaker and stirred for a time range of 5 to 15 min

and a stirring speed of 150–300 revolutions per minute (rpm). All the dispersions obtained were allowed to settle and the clarified samples were recovered from the top of the beaker for analysis. Following this, the clarified ones were removed for the analysis of the parameters: pH, conductivity (μS/cm), turbidity in nephelometric turbidity units (NTU), Fe_T (mg/L), P_T (mg/L), COD (mg/L), and SO_4^{-2} (mg/L).

Fig. 2. *Jar test equipment for the co-treatment of acidic water (AW) and urban wastewater (UWW)*

Optimization design

The parameters chosen for the co-treatment of AW and UWW were optimized by adopting the RSM. This methodology is a second-order regression analysis used to predict the value of the dependent variables through the manipulation of the independent variables (Asaithambi et al., 2016) and the central composite design (CCD). The CCD is a two-level factorial design with (2^n) factorial points, ($2n$) axial points corresponding to the highest and lowest levels of the factors, and center points (n_c) corresponding to the intermediate level of the factors, where n is the number of factors. In this sense, the number of treatments (N) is calculated based on Equation 2 (Arami-Niya et al., 2012; Khuri and Mukhopadhyay, 2010).

$$N = 2^n + 2n + n_c \quad (2)$$

Where: 2^n – factorial points; $2n$ – axial points; n_c – center points.

Response surface method (RSM)

For the experimental design, the CCD was selected with 3 factors and 2 levels (–1 and +1), 2 replicates, 6 axial points, 6 central points where the manipulated factors were the Fe/P molar ratio (X_1): (effect of the molar ratio), the stirring time (X_2): (effect of contact time) and the stirring speed (X_3): (effect of rapid mixing), as shown in *Table 1*.

The response variables chosen were pH, conductivity, turbidity, removal of COD, Fe_T, SO_4^{-2} and P_T. The values taken into account were chosen based on previous works related to co-treatment (Masindi et al., 2022; Ruihua et al., 2011; Spellman Jr et al., 2020).

Table 1. *Independent factors and their levels in the central composite design*

Factor	Variables	Levels		
		–1	0	+1
X_1	Molar ratio (mmol Fe/mmol P)	25	32.5	40
X_2	Stirring time (min)	5	10	15
X_3	Stirring speed (rpm)	150	225	300

Desirability function

The desirability function is a technique that determines the optimal conditions in a process based on the derringer desirability function (Asfaram et al., 2015). The derringer desirability function was applied for the simultaneous optimization of three operating parameters that influence the co-treatment of AW and UWW wastewater: Fe/P ratio, stirring time and stirring rate. The technique is applied because there are several factors with uncertainty and how they affect the quality of the treated water. The objective was to maximize the molar ratio, minimize the stirring time and stirring speed in the co-treatment of wastewater. The quality parameters of the treated water: pH, turbidity, chemical oxygen demand (COD), sulfates (SO_4^{-2}), total Iron (Fe_T) and total phosphorus (P_T).

Analytical instruments and techniques

All chemical products for the respective analyses were of analytical grade, being the analytical techniques

used to determine the quality parameters: pH (APHA, 2017, OACTON PCD650); electrical conductivity (APHA, 2017, multiparameter OACTON PCD650); turbidity (APHA, 2017, turbidimeter LOVIBOND T3250WL); COD (5220 D, closed reflux colorimetric method, colorimeter HACH DR900); total iron (Fe_T) (3500-FeB method, 1-10-phenanthroline spectrophotometer UV); sulfates ($SO4^{-2}$) (turbidimetric method 4500-SO4-2 E); total phosphorus (P_T) (4500-PC vanadomolybdophosphoric acid colorimetric method 33, spectrophotometer UV HACH DR4000). All analyses were conducted in triplicate (n = 3).

Applied statistical model

For the analysis and processing of the data, the analysis of variance (ANOVA) was used (Gutiérrez and De la Vara, 2004). Subsequently, the efficiency of CCD was statistically compared using the coefficient of determination (R^2), the predictive correlation coefficient (predictive R^2), and the adjusted correlation coefficient (adjusted R^2). Equation 3 shows the second-order CCD model used (Hussin et al., 2019; Khuri and Mukhopadhyay, 2010).

$$y = \beta_0 + \sum_{i=1}^{k} \beta_i x_i + \sum_{i=1}^{k} \sum_{j>1}^{k} \beta_{ij} x_i x_j + \sum_{i=1}^{k} \beta_{ii} x_i^2 + \varepsilon \quad (3)$$

Where: y – the response variable; β_0 – a constant coefficient; β_j, β_{ij}, β_{jj} – the coefficient of linear regression, quadratic regression and interaction regression, respectively; x_i, x_j – the manipulated factors; ε – the error.

For the validation of the model, the analysis of the residues was carried out. All the assumptions were globally contrasted. The lack of normality of the residues indicates that the model is inappropriate or the existence of heteroscedasticity. To give the model acceptability of each answer, the *F* value and the *P* value were analyzed. The statistical tests were completed with the Design Expert 11 software with a degree of reliability of 95%.

Results and Discussion

Characterization of the samples

The characterization of the samples included the evaluation of the following parameters: pH; electrical conductivity; turbidity; COD; total iron, sulfates and total phosphorus, as shown in *Table 2*.

Table 2. *Physicochemical characteristics of acidic water (AW) and urban wastewater (UWW)*

Parameter	Unit	AW	UWW
pH	pH units	1.83 ± 0.24	6.86 ± 0.37
Electrical conductivity	µS/cm	1 625.00 ± 145.23	1 461.00 ± 52.3
Turbidity	NTU	23.07 ± 4.6	52.00 ± 23.91
Chemical oxygen demand	mg/L	530.00 ± 46.7	240.50 ±35.7
Total iron (Fe_T)	mg/L	1 545.35 ± 120.3	0.898 ± 0.31
Sulphates (SO_4^{-2})	mg/L	6 260.60 ± 1 517.5	143.30 ± 48.9
Total phosphorus (P_T)	mg/L		8.287 ± 2.36

All the samples were analyzed in triplicate (n = 3)

Factors that affect the co-treatment of wastewater

Table 3 and *Table 4* show the results of the central composite design (CCD), from which the removal response values can be observed: COD (mg/L) from 68.3% (223 mg/L) to 73.04% (189.67 mg/L); total iron (mg Fe_T/L) from 98.53% (18.79 mg/L) to 99.88% (1.82 mg/L); total phosphorus (mg P_T /L) from 62.15% (1.84 mg/L) to 89.13% (1.07 mg/L) and sulfate (mg SO_4^{-2}/L) from 97.26% (715.03 mg/L) to 99.34% (124.38 mg/L), while the pH variability, turbidity (NTU) and conductivity (mS/cm) range from 4.28 to 6.53, from 4 to 204.5 and from 3.18 to 4.47, respectively.

Table 3. *CCD results with a set of 2^3, (n = 2), 6 axial points and 6 central points in the removal of contaminants*

Run	A	B	C	Response							
				COD removal		Fe_T removal		P_T removal		SO_4^{-2} removal	
	(mmol/ mmol)	(min)	(rpm)	mg/L	%	(mmol/ mmol)	%	(rpm)	%	mg/L	%
1	40	15	300	211.33 ± 1.46	69.96	18.59 ± 3.46	98.81	0.21 ± 0.07	73.04	715.03 ± 59.02	97.26
2	32.5	20	225	202 ± 2.83	71.28	18.79 ± 2.32	98.53	3.519 ± 0.08	77.87	217.84 ± 56.4	98.91
3	40	5	150	211.67 ± 2.36	69.91	7.1 ± 0.32	99.54	1.012 ± 0.08	82.11	458.88 ± 64.5	98.06
4	32.5	10	225	205 ± 4.95	70.86	6.19 ± 1.03	99.6	2.251 ± 0.16	77.87	261.16 ± 15.73	98.71
5	32.5	10	225	219.67 ± 3.77	71	5.34 ± 0.15	99.65	1.425 ± 0.23	78	297.16 ± 13.04	98.55
6	32.5	10	225	218.33 ± 3.06	70.91	5.24 ± 0.24	99.66	1.189 ± 0.11	78.54	205.09 ± 6.64	98.97
7	47.5	10	225	223 ± 5.23	68.3	13.01 ± 0.9	99.16	2.28 ± 0.08	78.64	328.95 ± 58.94	97.41
8	40	5	150	209.33 ± 1.29	70.24	8.46 ± 0.08	99.45	1.749 ± 0.1	87.07	238.43 ± 45.23	98.82
9	25	5	300	200.33 ± 7.16	71.52	5.98 ± 0.11	99.61	1.189 ± 0.15	85.82	147.55 ± 14.67	99.23
10	40	15	150	217.33 ± 83.56	71.1	13.82 ± 2.31	99.11	1.572 ± 0.13	68.27	408.7 ± 10.54	98.32
11	32.5	10	375	453.67 ± 10.34	71	7.3 ± 1.05	99.53	4.198 ± 0.25	69.33	281.01 ± 10.1	98.62
12	25	15	150	189.67 ± 1.88	73.04	7.48 ± 1.03	99.52	1.454 ± 0.35	69.39	448.79 ± 11.17	98.31
13	32.5	10	225	195 ± 6.36	71.28	4.57 ± 0.42	99.7	1.189 ± 0.23	76.28	537.75 ± 27.9	98.84
14	40	15	300	235 ± 5.87	68.59	15.14 ± 0.15	99.03	0.186 ± 0.03	76.87	435.1 ± 70.57	97.92
15	40	5	300	204.33 ± 2.99	70.95	12.94 ± 2.92	99.17	2.988 ± 0.09	84.17	325.07 ± 30.64	98.42
16	32.5	10	225	199.67 ± 7.54	71.61	4.69 ± 0.03	99.7	2.162 ± 0.16	76.28	302.06 ± 41.25	98.52
17	25	15	300	218.33 ± 4.72	68.96	7.76 ± 0.98	99.5	0.51 ± 0.08	76.81	256.94 ± 15.09	98.73
18	25	15	150	195.67 ± 6.31	72.18	4.99 ± 0.18	99.68	1.1 ± 0.04	73.18	280.88 ± 17.13	98.62
19	40	5	300	201 ± 7.78	71.42	11.27 ± 0.18	99.27	1.071 ± 0.06	89.13	370.29 ± 11.18	98.22
20	17.5	10	225	217 ± 3.89	69.15	1.82 ± 0.5	99.88	1.13 ± 0.11	79.65	178.27 ± 36.59	98.09
21	25	5	300	191.67 ± 1.65	72.75	8.25 ± 2.62	99.47	1.218 ± 0.15	88.07	130.37 ± 5.82	99.31
22	32.5	0	225	196.33 ± 2.1	72.09	15.66 ± 0.14	98.99	3.431 ± 0.18	87.09	211.89 ± 9.4	98.94
23	25	15	300	205.67 ± 3.27	70.76	11.51 ± 0.77	99.26	0.746 ± 0.1	78.05	124.38 ± 52.34	99.34
24	32.5	10	225	187.67 ± 3.73	71.12	6.33 ± 0.47	99.59	1.159 ± 0.15	77.23	204.75 ± 10.01	98.97
25	25	5	150	197.67 ± 2.64	71.9	8.14 ± 1.48	99.47	1.897 ± 0.18	73.28	583.53 ± 26.54	97.33
26	40	15	150	194 ± 1.91	72.85	11.46 ± 0.86	99.26	0.776 ± 0.14	73.28	658.61 ± 78.98	97.83
27	25	5	150	195.67 ± 3.73	72.18	1.95 ± 0.05	99.87	1.366 ± 0.19	70.92	425.63 ± 14.12	97.96
28	32.5	10	75	201 ± 10.54	71.82	7.08 ± 1.01	99.54	1.838 ± 0.28	62.15	459.47 ± 25.58	97.8

A: mmol Fe_T /mmol P_T, B: stirring time, C: stirring speed

Table 4. *CCD results with a set of 2^3, (n = 2), 6 axial points and 6 central points in the variation of physicochemical parameters*

Run	A	B	C	Response		
				pH	Turbidity	Conductivity
	(mmol/mmol)	(min)	(rpm)	pH unit	(NTU)	(mS/cm)
1	40	15	300	5.03 ± 0.17	27.5 ± 1.27	4.35 ± 0.07
2	32.5	20	225	5.51 ± 0.01	193.4 ± 1.06	4 ± 0.01
3	40	5	150	5.11 ± 0.26	25.7 ± 0.4	4.06 ± 0.01
4	32.5	10	225	5.85 ± 0.33	48.7 ± 0.81	3.84 ± 0.08
5	32.5	10	225	5.85 ± 0.35	46.2 ± 0.82	3.82 ± 0.03
6	32.5	10	225	5.9 ± 0.02	54.8 ± 1.98	3.74 ± 0.04
7	47.5	10	225	4.28 ± 0.06	4 ± 0.17	4.47 ± 0.03
8	40	5	150	5.01 ± 0.04	15.1 ± 0.65	4.15 ± 0.01
9	25	5	300	6.08 ± 0.03	77.3 ± 5.35	3.55 ± 0.01
10	40	15	150	5.06 ± 0.27	116.6 ± 1.61	4.27 ± 0.01
11	32.5	10	375	5.81 ± 0.08	165.6 ± 2.05	3.91 ± 0.02
12	25	15	150	6.02 ± 0.09	110.7 ± 1.7	3.57 ± 0.02
13	32.5	10	225	5.76 ± 0.02	40 ± 1.32	3.76 ± 0.01
14	40	15	300	4.89 ± 0.01	16.2 ± 0.88	4.35 ± 0.15
15	40	5	300	5.12 ± 0.01	38.6 ± 0.58	4.19 ± 0.03
16	32.5	10	225	5.78 ± 0.05	48.3 ± 1.08	3.88 ± 0.01
17	25	15	300	6.21 ± 0.05	94.6 ± 0.82	3.62 ± 0.02
18	25	15	150	6.06 ± 0.01	113.1 ± 4.57	3.56 ± 0.01
19	40	5	300	5.12 ± 0.01	22.2 ± 0.33	4.17 ± 0.01
20	17.5	10	225	6.53 ± 0.01	51.1 ± 2.34	3.18 ± 0.02
21	25	5	300	6.21 ± 0.22	129.1 ± 1.41	3.5 ± 0.06
22	32.5	0	225	5.6 ± 0.05	141.7 ± 3.54	3.8 ± 0.08
23	25	15	300	6.19 ± 0.01	103.9 ± 0.99	3.61 ± 0.02
24	32.5	10	225	5.67 ± 0.02	59 ± 1.56	3.91 ± 0.01
25	25	5	150	6.12 ± 0.34	37.2 ± 3.45	3.54 ± 0.01
26	40	15	150	5.16 ± 0.01	172.6 ± 2.5	4.34 ± 0.02
27	25	5	150	6.04 ± 0.01	26.3 ± 1.39	3.63 ± 0.02
28	32.5	10	75	5.65 ± 0.14	204.5 ± 4.03	4.28 ± 0.02

A: mmol Fe_T/mmol PT, B: stirring time, C: stirring speed

Table 3 shows that the Fe_T/P_T molar ratio influences the pH of the sample; it is shown when Fe_T/P_T molar ratio increases, the pH value decreases, resulting in high concentrations of iron, sulfate and a high conductivity in the sample. This indicates that the pH is one of the variables that determine the precipitation, flocculation and/or adsorption process, with a higher concentration of Fe_T and other metallic ions present in AW at lower pH (Masindi et al., 2022; Ruihua et al., 2011). The results show that the co-treatment process achieved a maximum Fe_T removal of 99.88% (1.82 mg/L) at a molar ratio of 17.5 (mmol Fe_T/mmol P_T), stirring time of 10 min and stirring speed of 225 rpm. This is similar to the results obtained in the research of Masindi et al. (2022), and is greater than the one obtained by Younger and Henderson (2014) with an 89% removal.

Fig. 3a and *Fig. 3b* show that the treatment achieves a maximum pH of 6.53 and Fe_T removal (> 98%), at a molar ratio of 17.5 (mmol Fe_T/mmol P_T), stirring time of 10 min and stirring speed of 225 rpm. It can be seen that the lowest Fe/P molar ratio and the final pH increases depend on the initial concentrations of Fe and pH of the AW. Similarly, at pH > 5, precipitation is more effective, since the phosphate species are found as orthophosphates and react with the iron, forming small colloidal particles that coagulate and start to precipitate, and then co-precipitate other complex compounds such as ferric-hydroxy phosphates, reflecting on a lower conductivity (3.18 mS/cm), with respect to the values of 256 mS/cm obtained by Masindi et al. (2022).

Fig. 3c illustrates that the turbidity increases slightly when the volumetric ratio decreases, which means that having lower availability of iron, the probability of interaction is lower between the species present in the wastewater, reflected in a greater turbidity. However, at stirring speed (> 220 rpm), the turbidity decreases due to a better contact between the particles that allows the interaction between them. Likewise, it is observed that the turbidity reached the highest efficiency of 22.2 NTU (57%) at a molar ratio of 40 (mmol Fe_T/mmol P_T), stirring time of 10 min and stirring speed of 225 rpm (Rao et al., 1992).

Fig. 4a shows that COD removal tends to increase when the molar ratio decreases, increasing the volume of UWW, which promotes the increase in pH and the subsequent precipitation of metals, reducing the COD to values of 189.67 mg/L at a molar ratio of 25 (mmol Fe_T/mmol P_T), stirring time of 15 min and stirring speed of 150 rpm, which are similar to those obtained by Masindi et al. (2022).

Fig. 4b shows a high removal of Fe_T (> 98%) that increases as the molar ratio is reduced (which translates into greater volumes of UWW with respect to AW), being indifferent to time and stirring speed. These removal mechanisms depend on several factors such as initial concentration, metal load and average pH (Hughes and Gray, 2013). In the same way, Strosnider et al. (2011) mention that the removal of Fe_T is produced by the increase in pH, where the solubility of the metals decreases, forming small colloidal particles which grow and precipitate through reaction mechanisms with phosphate $Fe(PO_4).2H_2O$, $Fe_3(PO_4)_2$, and $Fe(OH)_3$, precipitate other complex compounds such as oxyhydrophosphate as a result of variable concentrations of phosphate, orthophosphate and pH, generating ions and organic phosphorus in the formed flocs, corroborating what Masindi et al. (2022) indicates.

Fig. 4c shows that the highest percentages of P_T removal happens at a higher Fe_T/P_T molar ratio, short stirring time and high stirring speeds, given that with the greater availability of Fe^{+3}, due to its high charge, it has a higher affinity with PO_4^{-3} to form precipitates as $FePO_4$ (Dobbie et al., 2009; Masindi et al., 2022; Parsons and Smith, 2008; Ruihua et al., 2011). Besides, Johnson and Younger (2006) make reference that phosphate can be removed by precipitates of iron oxyhydroxide, as well as other phosphate salts (Alley, 2010; Ruihua et al., 2011). For this research, it was obtained a P_T removal of 89.13% for a molar ratio of 40 (Fe/P), at a stirring time of 15 min and stirring speed of 300 rpm. *Fig. 4d* shows how the removal of SO_4^{-2} decreases slightly as the molar ratio increases at stirring times greater than 10 min. This is explained by the fact that the pH of the solution is more acidic, increasing the solubility of sulfates and phosphates (Li and Kang, 2021). In this way, the concentration of SO_4^{-2} increases as the dose of AW increases. However, high percentages of SO_4^{-2} removal (> 97%) were obtained, due to the high concentration of Fe^{+3} and the presence of other metallic ions such as Al^{+3}, Ca^{+2} y Pb^{+2}, which would form precipitated as sulfates such as Fe and Al oxyhydrosulfates (Masindi et al., 2022; Ruihua et al., 2011).

Fig. 3. *3D response surface plots for the effects of molar ratio and stirring time in a) pH units, b) conductivity (mS/cm), c) turbidity (NTU)*

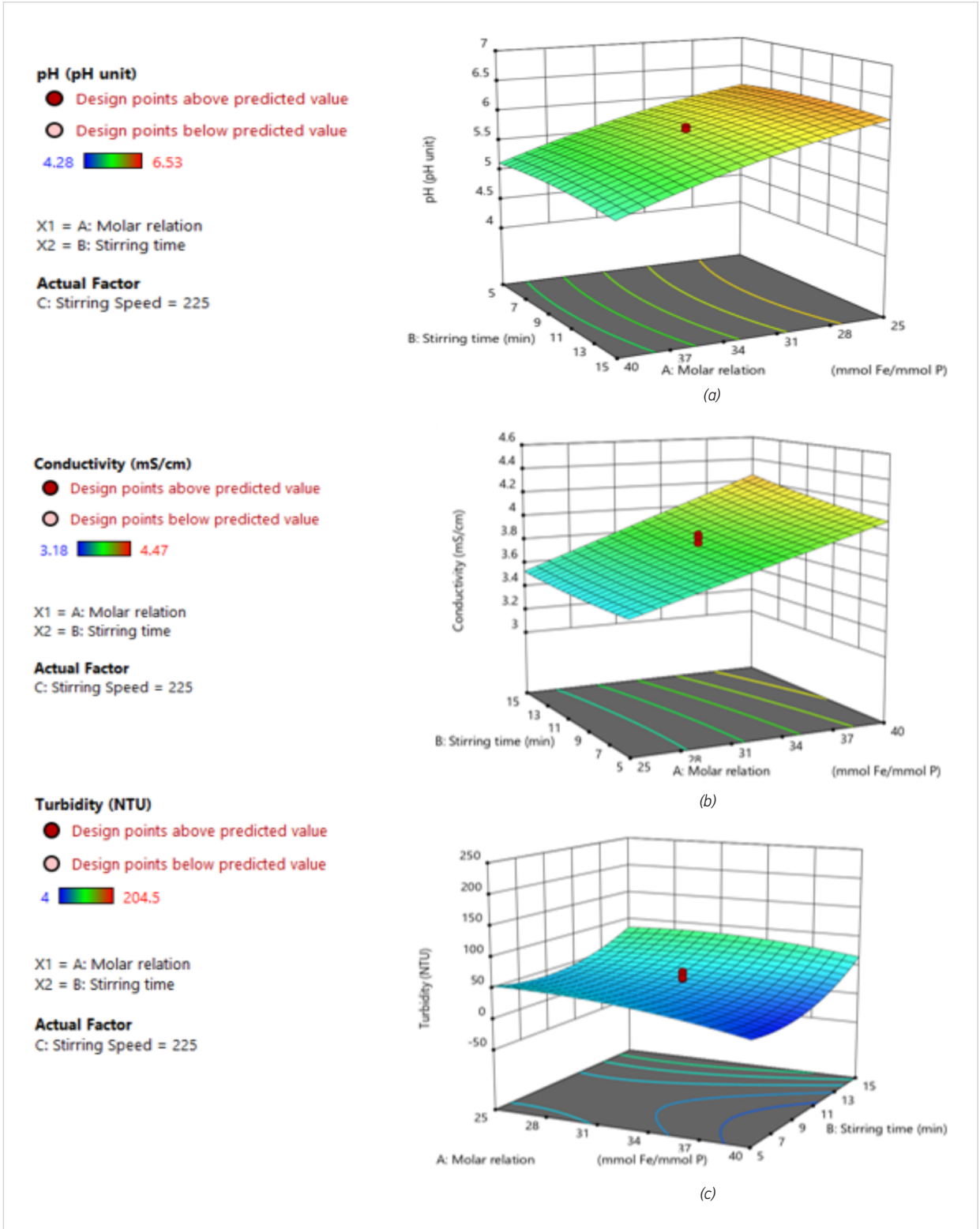

Fig. 4. *3D response surface plots for the effects of molar ratio and stirring time in a) COD removal (%), b) Fe_T removal (%), c) P_T removal (%), d) $SO4^{-2}$ removal (%)*

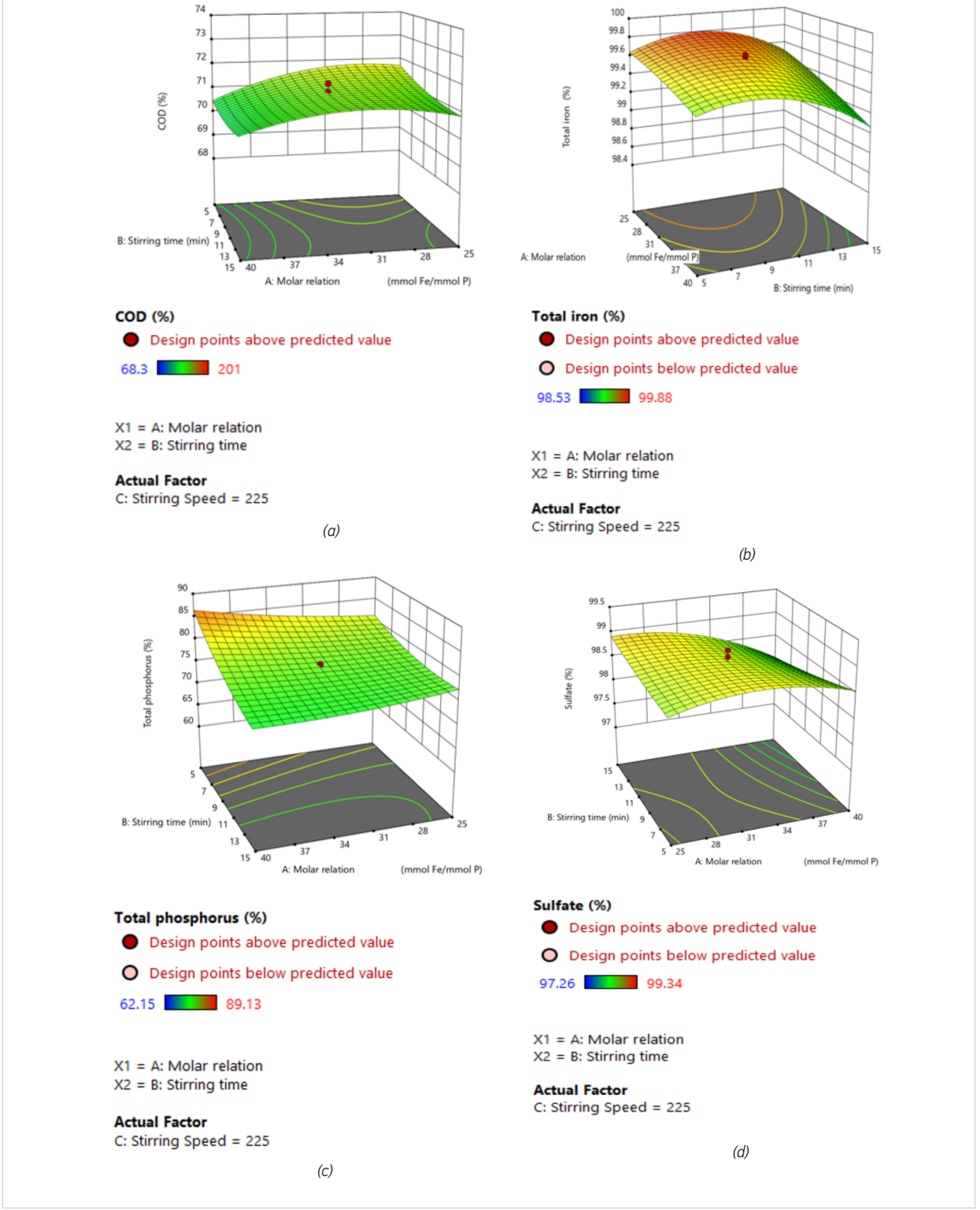

Table 5 shows a comparison of the values of pH and removal of Fe_T, P_T, COD and SO_4^{-2} with other research based on the co-treatment of AW and UWW, complementing with different treatment methods. The reported research of Deng and Lin (2013) and Masindi et al. (2022) show similar results to those in this research with removal values of iron and phosphorus of 99%.

Analysis of variance (ANOVA) of the model

Table 6 shows the summary results of the predictive model for each response variable. Regarding the significance of each factor, it was obtained that: X_1, X_1^2 and X_2^2 were significant in terms of pH; X_1, X_2 and X_3^2 were significant for conductivity; regarding turbidity, the significant factors were X_1, X_2, X_1X_3, X_2X_3, X_2^2 and X_3^2; for the removal in % of COD, X_1, X_3, X_2X_3, X_1^2 were significant; for the removal in % of total iron (Fe_T), X_1, X_2, X_3, X_1X_2, X_1X_3 and X_2^2 were significant; for the removal in % of phosphorus (P_T), X_2, X_3, X_1X_2, X_1X_3, X_2^2 and X_3^2 were significant; and for the removal in % of sulfates ($SO4^{-2}$), X_1, X_3, X_1X_2, X_1X_3, X_2X_3, X_1^2 y X_3^2 were significant.

The acceptance of the models for the response variables was analyzed using the *F* value and *P* value (*Table 7*) using the regression coefficient R^2, adjusted R^2, predictive R^2 and adequate precision.

Table 8 shows that the highest R^2 obtained for pH, conductivity and Fe_T removal were 0.9853, 0.9658 and 0.9219, respectively. The R^2 value obtained for Fe_T in this study was higher than that obtained in the research carried out by Núñez-Gómez et al. (2017), where they obtained a value $R^2 = 0.88$ but still indicated a high degree of correlation between the response and the independent variables in its central composite design.

Likewise, the adjusted R^2 values were 0.9780 (pH), 0.9486 (conductivity) and 0.8828 (Fe_T removal). As for the R^2 predictive, these resulted in 0.9651 (pH), 0.8842 (conductivity) and 0.776 (Fe_T removal). The difference of these indicators is within a margin of 0.20, which indicates a reasonable agreement for the proposed model.

Regarding the other response variables, such as turbidity, COD removal, P_T and SO_4^{-2}, the R^2 values were 0.8556, 0.8015, 0.8530 and 0.8396, respectively. This last value of R^2 for sulfate is similar to that obtained in the study by Pratinthong et al. (2021) who obtained an $R^2 = 0.8379$ in the research of removal of sulfates by precipitation of ettringite in which chemical reagents were applied. The R^2 was a desirable value and it fitted well to the evaluated quadratic model, as well as the R^2 obtained in this research was adjusted to the proposed quadratic model.

Table 5. *Comparison of contaminant removal results with other studies of co-treatment of AW and UWW*

Research topic	Pollutants removal					Reference
	pH	Fe_T	P_T	SO_4^{-2}	COD	
Co-treatment of acid mine drainage and municipal wastewater	5.1	99%	99%	93%	16%	Masindi et al., 2022
Co-treatment with secondary municipal wastewater with mine drainage	6	50%	> 90%		< 10%	Spellman Jr et al., 2020
Synergistic treatment of wastewater and mine water wetlands	-	89%	46%	-	-	Younger and Henderson, 2014
Combined two-stage treatment of acid mine drainage and municipal wastewater with aerobic mixing and anaerobic treatment	6.2–7.9	99%	99%	> 80%		Deng and Lin, 2013
Co-treatment of acid mine drainage with municipal wastewater with activated sludge		74–86 %	79%		87–93%	Hughes and Gray, 2013
Co-treatment of wastewater and mine water in aerobic wetlands		40-80%	10-50%			Johnson and Younger, 2006

Table 6. *ANOVA for the composite central design (CCD) of the physicochemical parameters*

Description	pH					Conductivity					Turbidity				
	DF	SS	MS	*F* value	*P* value	DF	SS	MS	*F* value	*P* value	DF	SS	MS	*F* value	*P* value
Model	9	7.33	0.8145	134.212	< 0.0001	9	2.832	0.315	56.406	< 0.0001	9	76604.48	8511.609	10.968	< 0.0001
X_1	1	6.945	6.9445	1144.34	< 0.0001	1	2.603	2.604	466.65	< 0.0001	1	5455.34	5455.341	7.03	0.0162
X_2	1	0.005	0.0051	0.841	0.3712	1	0.069	0.07	12.4538	0.0024	1	10287.49	10287.49	13.257	0.0019
X_3	1	0.015	0.0148	2.444	0.1354	1	0.011	0.011	1.9026	0.1847	1	1286.12	1286.12	1.657	0.2143
X_1X_2	1	0.004	0.0041	0.678	0.4209	1	0.022	0.022	4.0061	0.0606	1	297.74	297.74	0.384	0.5434
X_1X_3	1	0.025	0.0248	4.088	0.0583	1	0.004	0.004	0.6927	0.4162	1	7777.48	7777.48	10.022	0.0053
X_2X_3	1	0.004	0.0039	0.644	0.4328	1	0.001	0.001	0.2476	0.6248	1	11219.58	11219.58	14.458	0.0013
X_1^2	1	0.277	0.2771	45.659	< 0.0001	1	0	0	0.0013	0.9714	1	3078.67	3078.67	3.967	0.0618
X_2^2	1	0.112	0.1119	18.442	0.0004	1	0.008	0.008	1.386	0.2544	1	14780.85	14780.85	19.047	0.0004
X_3^2	1	0.012	0.0123	2.033	0.171	1	0.115	0.115	20.5778	0.0003	1	20653.28	20653.28	26.615	< 0.0001
Residual	18	0.109	0.0061			18	0.1	0.006			18	13968.24	776.013		
Lack of fit	5	0.041	0.0082	1.547	0.2426	5	0.065	0.013	4.7256	0.0111	5	9948.64	1989.727	6.435	0.0032
Error	13	0.068	0.0053			13	0.036	0.003			13	4019.6	309.2		
Total	27	7.439				27	2.933				27	90572.71			

Note: DF – degrees of freedom; SS – sum of squares; MS – mean squares

Table 7. *ANOVA for the CCD of the removal parameters*

Model	COD					Fe_T				
	DF	SS	MS	*F* value	*P* value	DF	SS	MS	*F* value	*P* value
	9	32.6	3.63	8.078	< 0.0001	9	2.304	0.256	23.605	< 0.0001
X_1	1	4.15	4.15	9.243	0.007	1	0.561	0.561	51.719	< 0.0001
X_2	1	1.06	1.06	2.368	0.1412	1	0.19	0.19	17.526	0.0006
X_3	1	4.28	4.28	9.534	0.0063	1	0.073	0.073	6.728	0.0183
X_1X_2	1	0.72	0.72	1.594	0.2229	1	0.099	0.099	9.126	0.0073
X_1X_3	1	0.28	0.28	0.633	0.4366	1	0.05	0.05	4.614	0.0456
X_2X_3	1	11.1	11.1	24.685	< 0.0001	1	0.027	0.027	2.489	0.132
X_1^2	1	7.76	7.76	17.294	0.0006	1	0.032	0.032	2.914	0.105
X_2^2	1	0.92	0.92	2.052	0.1691	1	1.298	1.298	119.646	< 0.0001
X_3^2	1	0.38	0.38	0.838	0.372	1	0.025	0.025	2.346	0.143
Residual	18	8.08	0.45			18	0.195	0.011		
Lack of fit	5	2.28	0.46	1.023	0.4438	5	0.081	0.016	1.851	0.1719
Error	13	5.8	0.45			13	0.114	0.009		
Total	27	40.7				27	2.499			

Model	P_T					SO_4^{-2}				
	DF	SS	MS	*F* value	*P* value	DF	SS	MS	*F* value	*P* value
	9	964.5	107.17	11.608	< 0.0001	9	7.63	0.85	10.394	< 0.0001
X_1	1	7.47	7.475	0.81	0.3801	1	1.2	1.2	14.662	0.001
X_2	1	330.84	330.84	35.835	< 0.0001	1	0.05	0.05	0.591	0.452
X_3	1	191.64	191.64	20.757	0.0002	1	0.97	0.97	11.92	0.003
X_1X_2	1	53.89	53.886	5.837	0.0265	1	0.71	0.71	8.643	0.009
X_1X_3	1	58.15	58.15	6.299	0.0219	1	1.97	1.97	24.181	0
X_2X_3	1	6.45	6.445	0.698	0.4144	1	0.5	0.5	6.135	0.023
X_1^2	1	10.61	10.606	1.149	0.2979	1	1.73	1.73	21.179	0
X_2^2	1	55.87	55.871	6.052	0.0242	1	0.03	0.03	0.361	0.555
X_3^2	1	187.64	187.64	20.324	0.0003	1	0.53	0.53	6.534	0.02
Residual	18	166.18	9.232			18	1.47	0.08		
Lack of fit	5	93.44	18.689	3.34	0.037	5	0.19	0.04	0.382	0.852
Error	13	72.74	5.595			13	1.28	0.1		
Total	27	1130.7				27	9.1			

Note: DF – degrees of freedom; SS – sum of squares; MS – mean squares

Table 8. *Supplementary ANOVA results for the central composite design (CCD)*

Variable	pH	Conductivity	Turbidity	COD removal	Fe_T removal	P_T removal	SO_4^{-2} removal
R^2	0.9853	0.9658	0.8556	0.8015	0.9219	0.853	0.8386
R^2 adjusted	0.978	0.9486	0.7834	0.7023	0.8828	0.7795	0.7579
R^2 predicted	0.9651	0.8842	0.4881	0.4429	0.776	0.54	0.6231
Adequate accuracy	46.2181	29.5141	13.0204	10.8986	19.9844	16.4199	11.1482
Standard deviation	0.0779	0.0747	26.97	0.6701	0.1041	3.01	0.2856
Mean	5.63	3.89	77.99	71.03	99.4	77.44	98.43
Variance coefficient (VC %)	1.38	1.92	34.59	0.94	0.1	3.88	0.29

Meanwhile, the adjusted R^2 and predictive R^2 values were 0.7834 and 0.4881 for turbidity, 0.7023 and 0.4429 for COD removal, 0.7795 and 0.54 for P_T removal, and finally 0.7579 and 0.6231 for $SO4^{-2}$ removal. Adequate precision is an indicator that measures the range between the predicted data and the design points with the average prediction error (Davarnejad and Nasiri, 2017). A value greater than 4 indicates that the model obtained can be applied to the proposed spatial design (Hussin et al., 2019). The adequate precision for the 7 response variables was greater than 4, which indicates that the quadratic model is adequate for the application of the CCD.

The following equations represent the CCD model obtained for the response variables. Using these Equations, the model predicts the value of the response variables based on the coded factors.

$$pH = 5.79 - 0.5379X_1 - 0.0146X_2 + 0.0249X_3 - 0.016X_1X_2 - 0.0394X_1X_3 - 0.0156X_2X_3 - 0.104X_1^2 - 0.0661X_2^2 - 0.022X_3^2 \quad (4)$$

$$Conductivity(uS/(cm^2)) = 3.82 + 0.3294X_1 + 0.0538X_2 + 0.021X_3 + 0.0374X_1X_2 + 0.0155X_1X_3 + 0.0093X_2X_3 - 0.005X_1^2 + 0.0174X_2^2 - 0.067X_3^2 \quad (5)$$

$$Turbidity(NTU) = 43.51 - 15.08X_1 + 20.7X_2 - 7.32X_3 + 4.31X_1X_2 - 22.05X_1X_3 - 26.48X_2X_3 - 10.97X_1^2 + 24.03X_2^2 - 28.4X_3^2 \quad (6)$$

$$COD(\%) = 71.23 - 0.4158X_1 - 0.2105X_2 + 0.4223X_3 + 0.2115X_1X_{(2)} + 0.1333X_1X_3 - 0.8233X_2X_3 - 0.5507X_1^2 + 0.1897X_2^2 0.1213X_3^2 \quad (7)$$

$$FeT(\%) = 99.65 - 0.1529X_1 - 0.089X_2 - 0.0551X_3 - 0.0787X_1X_2 - 0.0559X_1X_3 - 0.0411X_2X_3 - 0.0351X_1^2 - 0.2251X_2^2 - 0.0315X_3^2 \quad (8)$$

$$PT(\%) = 78.02 + 0.5581X_1 - 3.71X_2 + 2.83X_3 - 1.84X_1X_2 - 1.91X_1X_3 - 0.6347X_2X_3 + 0.6347X_1^2 + 1.48X_2^2 - 2.71X_3^2 \quad (9)$$

$$SO_4^{(-2)}(\%) = 98.75 - 0.2233X_1 - 0.0448X_2 + 0.2013X_3 - 0.2099X_1X_2 - 0.3512X_1X_3 - 0.01769X_2X_3 - 0.2598X_1^2 + 0.0339X_2^2 - 0.1443X_3^2 \quad (10)$$

Where: X_1, X_2 and X_3 are the parameters shown in *Table 2*.

In the case of COD, the residuals indicate how the model satisfies the assumptions of the ANOVA analysis, where the standardized residuals measure the differences between the observed values and the predicted values (Asaithambi et al., 2016). *Fig. 5* and *Fig. 6* show the normality of the residuals for the response variables. These graphs show that the data obtained follow a straight-line pattern; therefore, we can observe that the residuals have a normal distribution.

Fig. 5. *Plot of normality % probability vs. standardized residuals for a) pH, b) conductivity, c) turbidity*

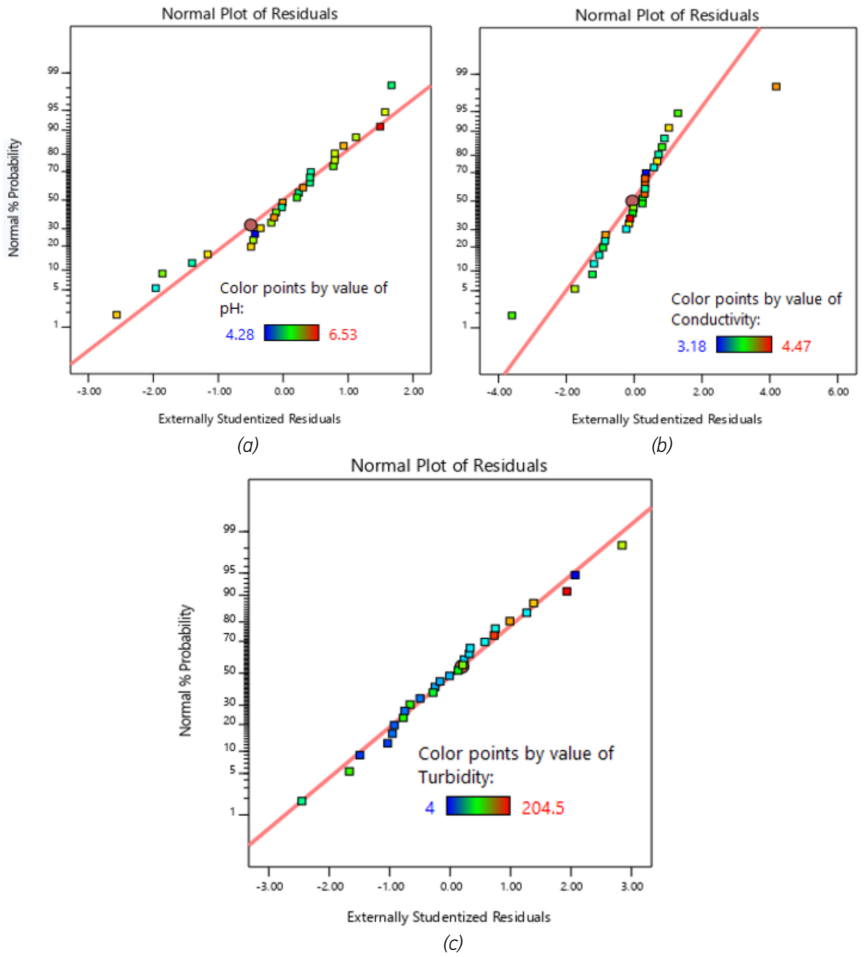

Fig. 6. *Plot of normality % probability vs. standardized residuals for a) COD removal, b) Fe_T removal, c) P_T removal, d) SO_4^{-2}removal*

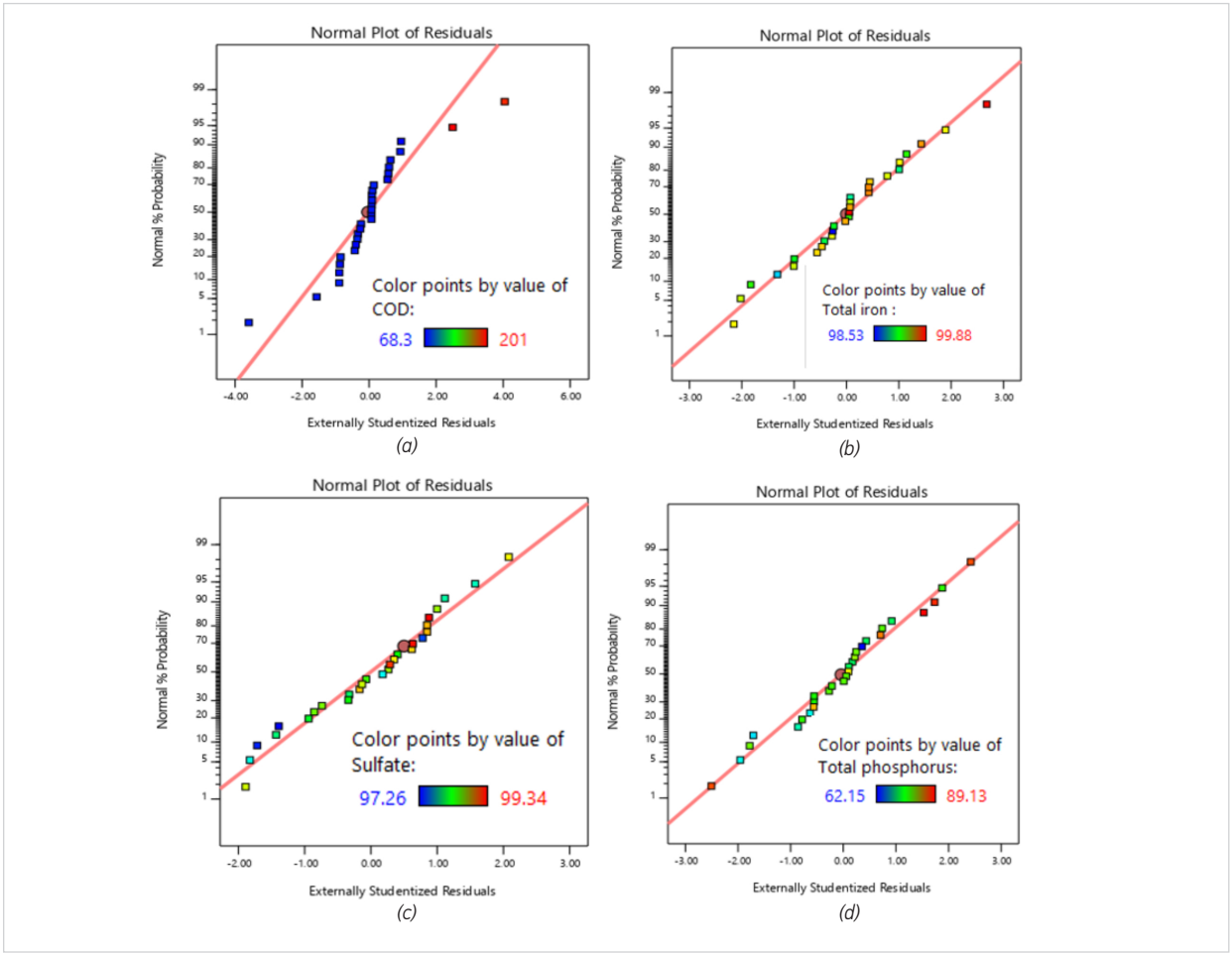

Optimization model

The objective of the optimization of the co-treatment for the AW of the Quiulacocha lagoon implies a good control of the operative conditions to achieve a balance between a better removal efficiency of water quality parameters and the low costs of the process. In general, operating costs are proportional to factors such as UWW supply, as well as the operating time required. In the particular case of this investigation, these factors are represented by the molar ratio (Fe_T/P_T), the stirring time and the stirring speed. For this, numerical optimization was used through the RSM to determine the optimal values of the factors to reach the maximum pH, the minimum conductivity, turbidity and the maximum removal of COD, Fe_T, P_T and SO_4^-.

To optimize the co-treatment conditions, the minimum possible value of the stirring time and the maximum of the molar ratio (Fe_T/P_T) were established, for a lower need for UWW. The stirring speed value was kept in the range (150–300 rpm). Regarding the response variables, the pH and the removal of COD, Fe_T, P_T and $SO4^{-2}$ were maximized. Meanwhile, the conductivity and turbidity were established at their minimum values.

Fig. 7 shows the optimization graph for the co-treatment of AW and UWW at a stirring speed of 255 rpm. The yellow part of the graph represents the values of the response variables that can be accepted. This range was at a molar ratio (Fe_T/P_T) between 20 and 40, with a stirring time between 5 and 20 min. In this sense, the optimal treatment was chosen based on the experimental runs with the highest desirability. This value is within a range from 0 to 1, with 1 being

Fig. 7. *Optimization chart for co-treatment*

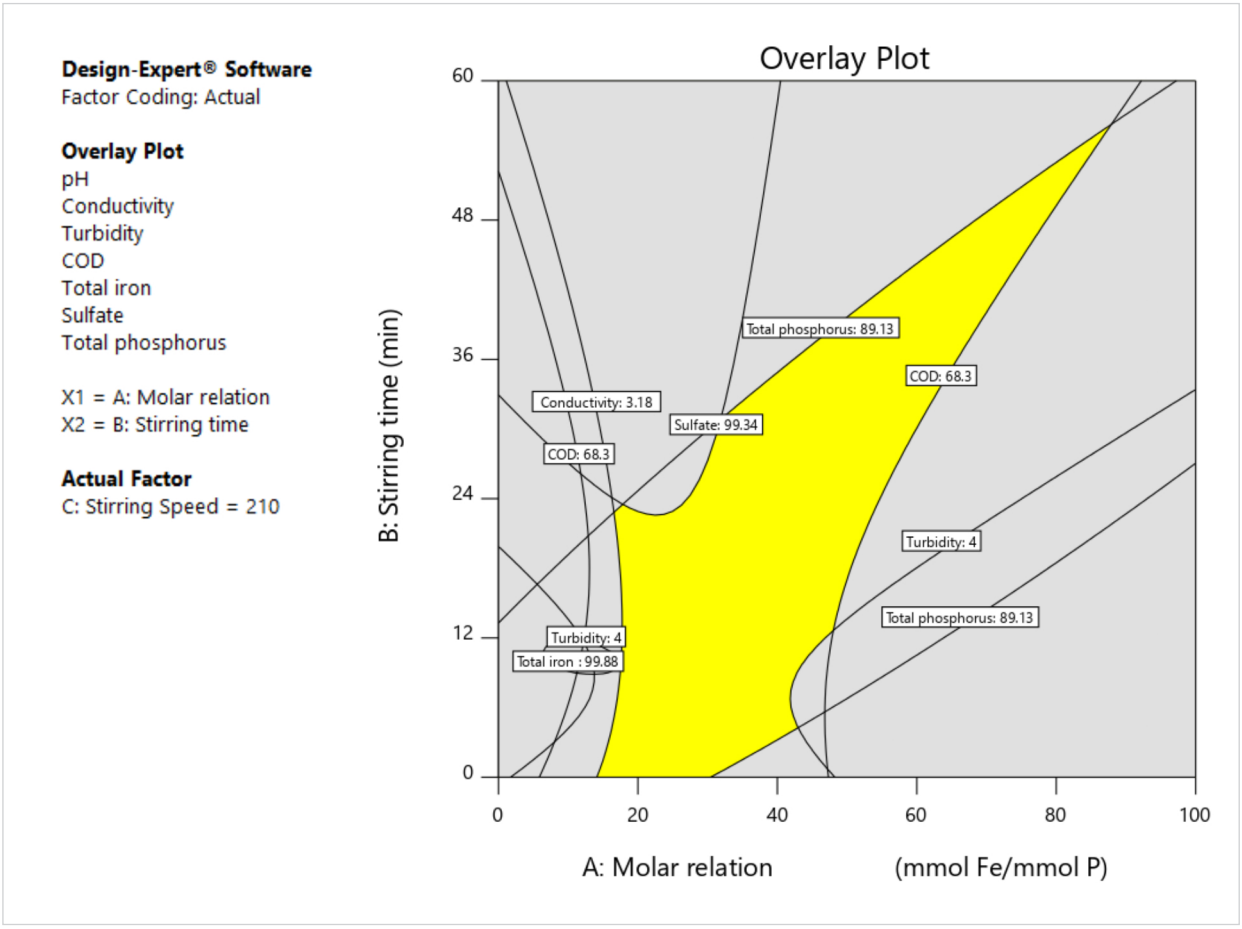

the value for the most desirable response and 0 for an undesirable response. The optimal treatment is shown in *Fig. 7* with a desirability of 0.71. This condition was given at a molar ratio (Fe_T/P_T) of 32.9, a stirring time of 5 min and a stirring speed of 255 rpm. In this way, a pH of 5.7, a conductivity of 3.8 mS/cm^2, a turbidity of 56 NTU, a removal of COD, Fe_T, P_T and SO_4^{-2} of 71.78%, 99.49%, 84.29% and 98.94% were obtained, respectively.

Conclusions

In this research, RSM was used for the optimization of the operating conditions of the co-treatment of AW and UWW such as the molar ratio (Fe_T/P_T), the stirring time and the stirring speed. The proposed CCD model provides a satisfactory level of prediction for the increase in pH, reduction in conductivity and reduction in total iron (mg Fe_T/L) with significant values of $P = 0.000$, with the factor X_1 = molar ratio (mmol Fe_T / mmol P_T) being the most significant. The proposed quadratic model resulted in an $R^2 > 0.92$ for the responses: pH, conductivity (mS/cm) and Fe_T removal (%). Likewise, an $R^2 > 0.80$ was obtained for turbidity (NTU) and removal of COD, total phosphorus (%) and sulfate (%).

The optimal conditions determined by the model were as follows: molar ratio 32.9:1 (mmol Fe_T / mmol P_T), stirring time of 5 min and a speed of 255 rpm. The pH reached a value of 5.7, the conductivity was 3.8 mS/cm^2, the turbidity was obtained at 56 NTU, the removal efficiencies of COD, Fe_T, P_T, SO_4^{-2} and their

residual values were 71.78% (198.5 mg/L), 99.49% (7.88 mg/L), 84.29% (1.3 mg/L) and 98.94% (474.15 mg/L), respectively.

This research demonstrated the effectiveness of co-treatment of AW from the Quiulacocha lagoon and UWW from Independencia municipality by developing a second-order model, and the importance of experimental design for optimizing operating conditions since it provides the conditions in which the greatest removal of contaminants would be obtained, taking into account that the molar ratio is a significant factor and that optimizing this factor would allow the co-treatment to be replicated in other polluted areas.

Regarding pH, this parameter does not exceed the water quality standards established by Peruvian regulations. Besides, all measurements were made after 30 min of rest after the jar test. Therefore, the use of a post-treatment is recommended for the regulation of the pH and the decrease in conductivity, as well as an increase in the rest time.

The co-treatment between AW and UWW is a promising alternative for the treatment of both types of water, which allows the reduction of costs since the additional use of chemical agents for the neutralization of AW is avoided. However, this alternative is not yet applied on a larger scale due to the high dose of residual water that is required; nevertheless, this represents a very promising pre-treatment alternative that, when coupled with other subsequent technologies, would achieve better efficiency. In addition, this co-treatment can be used using those wastewaters with high concentrations of PO_4^{-3} that are close to mining areas to reduce the costs of supplying wastewater.

On the other hand, regarding the limitation of the research, analytical techniques such as SEM/FIB/EDX, FTIR and XRD were not applied, despite the fact that these would have allowed a better understanding of the reaction mechanisms of the synergism between the AW and UWW. However, the aim of the research was to optimize the iron-phosphorus ratio, which are the main components of the treated water.

Finally, it is recommended to use other residues that contain a high phosphorus content allowing the removal of iron from AW, favoring the principle of circular economy.

Acknowledgements

This research was financed by CONCYTEC-PROCIENCIA, within the framework of the call E041-01 with Award Contract No. 178-2018-FONDECYT-BM-IA-DT-AV. Also, we would thank the Central Institute of Research, Science and Technology (ICICyT) and the Faculty of Environmental Engineering and Natural Resources of the National University of Callao.

References

Alley, E. (2010). Water Quality Control Handbook. McGraw-Hill Professional.

ANA. (2016). R.J. No 010-2016-ANA. Available at: http://www.ana.gob.pe/normatividad/rj-no-010-2016-ana-0 (accessed 13 February 2023).

Arami-Niya, A., Wan Daud, W. M. A., S. Mjalli, F., Abnisa, F. and Shafeeyan, M. S. (2012). Production of microporous palm shell based activated carbon for methane adsorption: Modeling and optimization using response surface methodology. Chemical Engineering Research and Design, 90(6), 776-784. https://doi.org/10.1016/j.cherd.2011.10.001

Asaithambi, P., Aziz, A. R. A. and Daud, W. M. A. B. W. (2016). Integrated ozone-electrocoagulation process for the removal of pollutant from industrial effluent: Optimization through response surface methodology. Chemical Engineering and Processing: Process Intensification, 105, 92-102. https://doi.org/10.1016/j.cep.2016.03.013

Astete, J., Cáceres, W., Gastañaga, M. del C., Lucero, M., Sabastizagal, I., Oblitas, T., Pari, J. and Rodríguez, F. (2009). Intoxicación por plomo y otros problemas de salud en niños de poblaciones aledañas a relaves mineros. Revista Peruana de Medicina Experimental y Salud Publica, 26(1), 15-19.

Batista, K., Lautert-dutra, W. and Carneiro, T. (2020). Acid mine drainage (AMD) treatment by neutralization: Evaluation of physical-chemical performance and ecotoxicological effects on zebra fish (Danio rerio) development. Chemosphere, 253, 1-11. https://doi.org/10.1016/j.chemosphere.2020.126665

Carneiro Brandão, T. C., Batista dos Santos, K., Lautert-Dutra, W., de Souza Teodoro, L., de Almeida, V. O., Weiler, J., Homrich Schneider, I. A. and Reis Bogo, M. (2020). Acid mine

drainage (AMD) treatment by neutralization: Evaluation of physical-chemical performance and ecotoxicological effects on zebrafish (Danio rerio) development. Chemosphere, 253, 126665. https://doi.org/10.1016/j.chemosphere.2020.126665

Baylón Coritoma, M., Roa Castro, K., Libio Sánchez, T., Tapia Ugaz, L., Jara Pena, E., Macedo Prada, D., Salvatierra Sevillano, A. and Dextre Rubina, A. (2018). Evaluación de la diversidad de algas fitoplanctónicas como indicadores de la calidad del agua en lagunas altoandinas del departamento de Pasco (Perú). Ecología Aplicada, 17(1), 119-132. https://doi.org/10.21704/rea.v17i1.1180

Calabi-Floody, M., Medina, J., Suazo, J., Ordiqueo, M., Aponte, H., Mora, M. de L. L. and Rumpel, C. (2019). Optimization of wheat straw co-composting for carrier material development. Waste Management, 98, 37-49. https://doi.org/10.1016/j.wasman.2019.07.041

Davarnejad, R., and Nasiri, S. (2017). Slaughterhouse wastewater treatment using an advanced oxidation process: Optimization study. Environmental Pollution, 223, 1-10. https://doi.org/10.1016/j.envpol.2016.11.008

Deng, D. and Lin, L.-S. (2013). Two-stage combined treatment of acid mine drainage and municipal wastewater. Water Science and Technology, 67(5), 1000-1007. https://doi.org/10.2166/wst.2013.653

Dobbie, K. E., Heal, K. V., Aumônier, J., Smith, K. a., Johnston, A. and Younger, P. L. (2009). Evaluation of iron ochre from mine drainage treatment for removal of phosphorus from wastewater. Chemosphere, 75(6), 795-800. https://doi.org/10.1016/j.chemosphere.2008.12.049

Dold, B., Wade, C. and Fontboté, L. (2009). Water management for acid mine drainage control at the polymetallic Zn-Pb-(Ag-Bi-Cu) deposit Cerro de Pasco, Peru. Journal of Geochemical Exploration, 100(2-3), 133-141. https://doi.org/10.1016/j.gexplo.2008.05.002

Edzai, W., Sheridan, C. and Rumbold, K. (2020). Global Co-occurrence of Acid Mine Drainage and Organic Rich Industrial and Domestic Effluent: Biological sulfate reduction as a co-treatment-option. Journal of Water Process Engineering, 38, 101650. https://doi.org/10.1016/j.jwpe.2020.101650

Gutiérrez, H. and De la Vara, R. (2004). Análisis y diseño de experimentos. McGraw-Hill Professional.

Hughes, T. and Gray, N. F. (2013). Co-treatment of acid mine drainage with municipal wastewater: performance evaluation. Environmental Science and Pollution Research, 20(11), 7863-7877. https://doi.org/10.1007/s11356-012-1303-4

Hussin, F., Aroua, M. K. and Szlachtac, M. (2019). Combined solar electrocoagulation and adsorption processes for Pb(II) removal from aqueous solution. Chemical Engineering and Processing - Process Intensification, 143, 107619. https://doi.org/10.1016/j.cep.2019.107619

Huzir, N. M., Aziz, M. M. A., Ismail, S. B., Mahmood, N. A. N., Umor, N. A. and Muhammad, S. A. F. S. (2019). Optimization of coagulation-flocculation process for the palm oil mill effluent treatment by using rice husk ash. Industrial Crops and Products, 139, 111482.https://doi.org/10.1016/j.indcrop.2019.111482

Johnson, K. L. and Younger, P. L. (2006). The co-treatment of sewage and mine waters in aerobic wetlands. Engineering Geology, 85(1-2), 53-61. https://doi.org/10.1016/j.enggeo.2005.09.026

Khuri, A. I. and Mukhopadhyay, S. (2010). Response surface methodology. Wiley Interdisciplinary Reviews: Computational Statistics, 2(2), 128-149. https://doi.org/10.1002/wics.73

Li, S. and Kang, Y. (2021). Effect of PO43- on the polymerization of polyferric phosphatic sulfate and its flocculation characteristics for different simulated dye wastewater. Separation and Purification Technology, 276(May), 119373. https://doi.org/10.1016/j.seppur.2021.119373

Masindi, V., Foteinis, S. and Chatzisymeon, E. (2022). Co-treatment of acid mine drainage and municipal wastewater effluents: Emphasis on the fate and partitioning of chemical contaminants. Journal of Hazardous Materials, 421(June 2021), 126677. https://doi.org/10.1016/j.jhazmat.2021.126677

Mavhungu, A., Masindi, V., Foteinis, S., Mbaya, R., Tekere, M., Kortidis, I. and Chatzisymeon, E. (2020). Advocating circular economy in wastewater treatment: Struvite formation and drinking water reclamation from real municipal effluents. Journal of Environmental Chemical Engineering, 8(4), 103957. https://doi.org/10.1016/j.jece.2020.103957

Montgomery, D. C. (2017). Design and analysis of experiments. John wiley and sons.

Muga, H. E. and Mihelcic, J. R. (2008). Sustainability of wastewater treatment technologies. Journal of Environmental Management, 88(3), 437-447. https://doi.org/10.1016/j.jenvman.2007.03.008

Naidu, G., Ryu, S., Thiruvenkatachari, R., Choi, Y., Jeong, S. and Vigneswaran, S. (2019). A critical review on remediation, reuse, and resource recovery from acid mine drainage. Environmental Pollution, 247, 1110-1124. https://doi.org/10.1016/j.envpol.2019.01.085

Núñez-Gómez, D., Lapolli, F. R., Nagel-Hassemer, M. E. and Lobo-Recio, M. Á. (2017). Optimization of acid mine drainage remediation with central composite rotatable design model. Energy Procedia, 136, 233-238. https://doi.org/10.1016/j.egypro.2017.10.248

Panić, S., Rakić, D., Guzsvány, V., Kiss, E., Boskovic, G., Kónya, Z. and Kukovecz, Á. (2015). Optimization of thiamethoxam ad-

sorption parameters using multi-walled carbon nanotubes by means of fractional factorial design. Chemosphere, 141, 87-93. https://doi.org/10.1016/j.chemosphere.2015.06.042

Parsons, S. A. and Smith, J. A. (2008). Phosphorus Removal and Recovery from Municipal Wastewaters. Elements, 4(2), 109-112. https://doi.org/10.2113/GSELEMENTS.4.2.109

Pratinthong, N., Sangchan, S., Chimupala, Y. and Kijjanapanich, P. (2021). Sulfate removal from lignite coal mine drainage in Thailand using ettringite precipitation. Chemosphere, 285, 131357. https://doi.org/10.1016/j.chemosphere.2021.131357

Ruihua, L., Lin, Z., Tao, T. and Bo, L. (2011). Phosphorus removal performance of acid mine drainage from wastewater. Journal of Hazardous Materials, 190(1-3), 669-676. https://doi.org/10.1016/j.jhazmat.2011.03.097

Schippers, A. (2007). Microorganisms involved in bioleaching and nucleic acid-based molecular methods for their identification and quantification. In Microbial processing of metal sulfides (pp. 3-33). Springer. https://doi.org/10.1007/1-4020-5589-7_1

Silva, D., Weber, C. and Oliveira, C. (2021). Neutralization and uptake of pollutant cations from acid mine drainage (AMD) using limestones and zeolites in a pilot-scale passive treatment system. Minerals Engineering, 170, 107000. https://doi.org/10.1016/j.mineng.2021.107000

Spellman Jr, C. D., Tasker, T. L., Strosnider, W. H. J. and Goodwill, J. E. (2020). Abatement of circumneutral mine drainage by Co-treatment with secondary municipal wastewater. Journal of Environmental Management, 271, 110982.https://doi.org/10.1016/j.jenvman.2020.110982

Strosnider, W., Winfrey, B. and Nairn, R. (2011). Novel passive co-treatment of acid mine drainage and municipal wastewater. Journal of Environmental Quality, 40(1), 206-213. https://doi.org/10.2134/jeq2010.0176

Talukdar, B., Kalita, H. K., Baishya, R. A., Basumatary, S. and Sarma, D. (2016). Evaluation of genetic toxicity caused by acid mine drainage of coal mines on fish fauna of Simsang River, Garo-hills, Meghalaya, India. Ecotoxicology and Environmental Safety, 131, 65-71.https://doi.org/10.1016/j.ecoenv.2016.05.011

Yang, C., Nan, J., Yu, H. and Li, J. (2020). Embedded reservoir and constructed wetland for drinking water source protection: Effects on nutrient removal and phytoplankton succession. Journal of Environmental Sciences (China), 87, 260-271. https://doi.org/10.1016/j.jes.2019.07.005

Younger, P. L. and Henderson, R. (2014). Synergistic wetland treatment of sewage and mine water: Pollutant removal performance of the first full-scale system. Water Research, 55(0), 74-82. https://doi.org/10.1016/j.watres.2014.02.024

Zhuang, P., McBride, M. B., Xia, H., Li, N. and Li, Z. (2009). Health risk from heavy metals via consumption of food crops in the vicinity of Dabaoshan mine, South China. Science of the Total Environment, 407(5), 1551-1561. https://doi.org/10.1016/j.scitotenv.2008.10.061